Research Article

ISSN: 2347-7385

HCCI Engine as chemical reactor to produce fuel/chemicals: An exploring study of n-alkanes low-temperature *ch*emistry in an HCCI Engine

Ahmad Saylam*

Institute for Combustion and Gas Dynamics, University of Duisburg-Essen: Lotharstraße 1, Raum: MA 363 - 47057 Duisburg - Germany

Asian Journal of Engineering and Technology Innovation. Volume 08 Issue 2

Published on: 11/12/2020

***Author for Correspondence:** Ahmad Saylam, University of Duisburg-Essen: Lotharstraße 1, Raum: MA 363 - 47057 Duisburg – Germany; Tel: +49 203 379 3543 - Fax: +49 203 379 8159; ahmad.saylam@uni-due.de

Cite this article as: Saylam A. *HCCI Engine as chemical reactor to produce fuel/chemicals: An exploring study of n-alkanes low-temperature chemistry in an HCCI Engine*. Asian Journal of Engineering and Technology Innovation, Vol 8(2), 1-12:2020.

ABSTRACT

The species production (oxygenated hydrocarbons, hydrogen peroxide, formaldehyde, and alkenes) of low-intermediate temperature (LIT) chemistry of C_1-C_7methane, ethane, propane, *n*-butane, *n*-pentane, *n*-hexane and *n*-heptane fuelled a homogeneous charge compression ignition (HCCI) combustion process was explored via single-zone modeling. At fixed intake temperature and pressure of 400 K and 1 bar and in varying compression ratio from 3 to 19, engine speed from 100 to 2000 rpm and equivalence ratio of investigated *n*-alkanes/air mixtures from 0.05 to 1, the main production of target species is generated under portions of LIT region, which starts at near 680 K to around 1000 K depending of *n*-alkane. This maximum production is attended during the maximum mixture reactivity near to Top Dead Center (TDC) and survive the remaining cycle when auto-ignition is avoided. The engine speed of 400 rpm is the favourite for the studied C_1-C_7 *n*-alkanes. Maximum productivity from longer-chain *n*-alkanes is less sensible toward engine speed variation. A compression ratio of 5 is near optimal for the top conversion of C_4-C_7 *n*-alkanes, but higher values are needed for the lower-reactivity alkanes of C_1-C_3. The intermediate reactivity of *n*-butane leads to a wide range of productive equivalence ratio reaching stoichiometry. The lower and higher-reactivity of other *n*-alkanes oblige leaner productive conditions, less than 0.5. The synthesis process of chemicals/reactive fuels blend using an HCCI engine with yields up to 85% for *n*-heptane, as primary chemical/fuel, is now theoretically justified and necessities indeed to be validated experimentally.

Key words: HCCI engine, cycle-to-cycle variability, low temperature chemistry, synthetic fuel/chemicals, fuel/product species

INTRODUCTION

Homogeneous charge compression ignition (HCCI) engine is low-temperature combustion (LTC) concept which combines the best features of conventional spark-ignition (SI) and compression-ignition (CI) engines [1]. However, an eventual commercially implementing of HCCI engines could be attended only after the overcoming of several challenges, especially solutions must be established to control ignition timing and expand its limited operating range [2]. The fully HCCI engine process controlling by the chemical kinetics is still the more thoughtful challenge, which means the directly affecting of the combustion process by the fuel composition, equivalence ratio, inlet conditions, the intermediate thermochemical state of the fuel–air mixture in oxidation, and the Residual gas (RG), which is a portion of exhaust gas from previous cycles stayed in cylinder and not purged during gas exchange, can be a source of cycle-to-cycle variability in HCCI engines. As well as the exhaust gas recirculation (EGR) through a dedicated external pathway from exhaust to intake which can be utilized in strategies to improve engine operation. The effect of controlled EGR quantities on HCCI engine performance was simulated by Chen el al. [3]. Agarwal et al. [4] studied the use of external EGR to introduce reactive mixtures to the cylinder. The products of the low-temperature combustion in an HCCI engine were fed to the intake of a Diesel engine to reduce its particulate matter and NOx emissions. The idea of reforming fuel in one cylinder and adding that exhaust gas to the intake of the other cylinders to improve their operating characteristics ("dedicated EGR") was introduced by Alger and Chadwell et al. [5, 6] for multi-cylinder SI engines. The paper of Tartakovsky et al. [7] discussed the fuel reforming in the context of internal combustion engines and also in an external catalytic reformer. Furthermore, the effects of temperature gradients inside the cylinder have high influence on the combustion process. The hottest part of the fuel-air mixture, located in the core of cylinder, ignites first to compress the rest of the mixture, which then ignites after a short time delay. In such system the crevices and boundary layers remain generally too cold to completely react, and so result in substantial hydrocarbon and carbon monoxide emissions. Therefore, the multi-zone

model for accurate predictions of HCCI combustion becomes a necessity in a condition to be coupled with fluid mechanic's simulation [8] and/or experimental evaluation of temperature distribution inside the combustion cylinder.

The usage of HCCI combustion process for producing base chemicals like ethene and synthesis gas (CO/H_2 mixtures) or alkenes together with some work and heat output under fuel-rich conditions has been recently explored under the idiom "polygeneration" [9-13]. However, useful chemicals/ synthetic fuels (oxygenated hydrocarbons, hydrogen peroxide, formaldehyde, and alkenes) could also be produced in the early stages of fuel-lean combustion [14, 15]. Such production could be usefully exploited if:

- The temperature reduction in the expansion stroke were timed right to avoid complete conversion of low-intermediate temperature (LIT) chemistry, so-called "cool flames", products of oxygenated hydrocarbons, hydrogen peroxide, formaldehyde and alkenes.
- The converting of such reactive species to carbon monoxide and carbon dioxide is also evaded during the compression stroke, by avoiding the pass to an auto-ignition regime of high temperature chemistry [15]. Yamada et al. [16] showed that such pass avoiding could be reached by suppressing the LIT chemistry attended by reducing the inter-cycles formation of hydrogen peroxide.

The modeling study of oxygenated hydrocarbons, hydrogen peroxide, and ethene formation from C_1–C_3 alkanes in an HCCI engine of Saylam et al. [15] could be considered as a modified view of the concept of "reactive coupling" that was a big topic 20 years ago [17, 18], attempting to find a kinetic way to convert the methane and alkanes in natural gas into "higher hydrocarbons", usually ethane. The rather new feature of the study [15] was the use of an HCCI engine as reactor in which this coupling was intended to occur. It has been recognized the very important role of reaction temperature in fuel ignition and also in lower temperature conversion of fuels to stable intermediate species. The difficulty was that methane, ethane, and propane are all fuels that do not participate to any significant amount of LIT reaction, via so-called "cool flame" reactions that produce large amounts of oxygenated intermediate species and *n*-alkenes. These species do not support cool flame oxidation reaction because the fuels are too small to support H atom transfer within the molecule that are key reaction pathways for larger fuel molecules. As a result, the three studied small fuel molecules react along well-known pathways to produce the main intermediates of ethene, hydrogen peroxide, and formaldehyde. These sensible results could "close that door" as a possible means of practical conversion of C_1-C_3 alkanes to larger hydrocarbons. Therefore, the aim of this study is to explore the same territory using much larger hydrocarbon fuels, C_4-C_7 *n*-alkanes, to produce useful oxygenated hydrocarbons and other intermediate species. The proposed optimization scheme by Saylam et al. [15] could not seem that is will reliably yield the optimum, due to the highly non-linear nature of fuel conversion with respect to fuel nature, equivalence ratio and the diversity of operating conditions. Nevertheless, it would be very helpful to focus the exploration of parameters ranges for the algorithms of multi-variable optimization scheme and also for the experimental validations. Therefore, this work has adopted that optimization scheme to determine the 'near optimal operating conditions' [15] of maximum target products yields.

In the LIT regime of combustion, hydrocarbons consumption occurs via H-atom abstraction, primarily by hydroxyl and hydroperoxyl radicals, and to a lesser extent by hydrogen and methyl radicals and oxygen molecular [19]. The oxidation chemistry of alkanes having at least four atoms of carbon involves isomerization reactions of peroxy radicals to give hydroperoxyalkyl radicals in the long alkyl chain that play an important role in the characteristics of LIT chemistry: auto-ignition in two stages, the appearance of the zone of negative temperature coefficient (NTC) [20], and oxygenated hydrocarbons, hydrogen peroxide, formaldehyde and alkenes main formation. A General oxidation mechanism between 600 and 1000 K for alkanes of Herbinet et al. [21] is presented in figure 1.

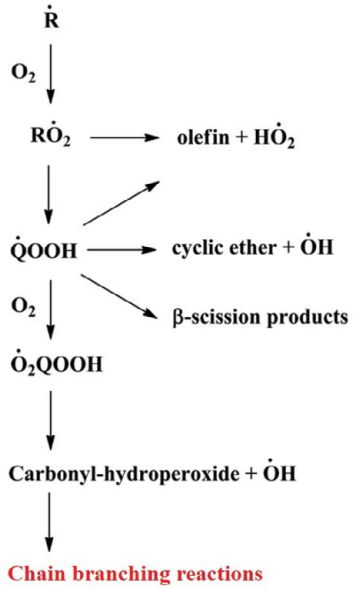

Figure 1: A General oxidation mechanism between 600 and 1000 K of alkanes (RH) [21], R˙, RO_2˙, ˙QOOH, $^{\cdot}O_2QOOH$ are alkyl radicals (derived from the initial alkane RH), peroxyalkyl radicals, hydroperoxyalkyl radicals and hydroperoxyalkylperoxy radicals, respectively.

Jet stirred reactors (JSRs) are frequently employed for studying homogeneous gas phase chemical kinetics of fuels. Therefore, their results could be very appropriated for this paper interests of LIT chemistry products under HCCI combustion process. Herbinet et al. [22] published an interesting study to understand the low temperature chemistry of *n*-alkanes (*n*-butane, *n*-hexane and *n*-heptane) using a JSR connected with gas chromatography to quantify the cyclic ethers, with mass spectrometry to detect hydroperoxides, including ketohydroperoxides, acids and compounds with two carbonyl functions, and optical diagnostics to identify hydrogen peroxide, and OH and HO_2 radicals. The coupling of a JSR by a continuous wave cavity ring-down spectroscopy (CRDS) in the near-infrared, effectuated by Bahrini et al. [23], permitted the quantification of hydrogen peroxide formed mainly in the range of 600-700 K of the low-temperature oxidation of a stoichiometric *n*-butane/oxygen/helium mixture.

The low-temperature oxidation of a stoichiometric *n*-butane/oxygen/argon mixture was analysed in a JSR by Herbinet et al. [24, 25]. The studied operating conditions were quasi-atmospheric pressure (0.105 MPa) and temperatures between 550 and 800 K. The formation of hydrogen peroxide, alkenes, aldehydes, cyclic ethers, hydroperoxides and ketohydroperoxide was detected generally at low temperature (< 800 K) with a maximum of fuel conversion of 47% at 630 K.

The *n*-pentane oxidation in a JSR at *p*= 1 and 10 atm, in the temperature range 500–1100 K, and for equivalence ratios of ϕ= 0.3–2.0 was studied by Bugler et al. [26]. It was observed, for ϕ= 0.5 and at *p*= 1 and 10 atm, the mainly formation of maximum mole fractions of oxygenated species was at low temperatures < 800 K, and that of *n*-alkenes was at intermediate temperature 800 – 1100 K. The pressure rising effect on these species formation manifested by a quit wider temperature ranges of maximum products formation but with decreasing in production concentration. The auto-ignition behaviour of the three pentane isomers was investigated by Kang et al. [14], under motored engine conditions of an intake temperature 393 K, a fixed engine speed 600 rpm and the lean conditions of ϕ= 0.25 and 0.5. At ϕ= 0.25, the maximum products of *n*-pentane oxidation of oxygenated hydrocarbons (aldehydes, ketones, cyclic ethers) and alkenes were identified around compression ratios of 6 and 7-8, respectively, which correspond to low and intermediate maximum temperature calculated from measured in-cylinder pressure. The pre-auto-ignition chemistry of *n*-pentane and 1-pentene was studied by Minetti et al. [27] in a rapid compression machine at the low temperature range 600–900 K. At the top dead center (TDC) conditions of temperature 733 K and pressure 6.9 bar, 11.5% of *n*-pentane has been converted to cyclic ethers where 2-methyltetrahydrofuran and oxetanes were the dominated products, and only 3.3% converted to 1-pentene. The major products from both hydrocarbons were C_2–C_4 aldehydes and ethanal, but *n*-pentane gave relatively large amounts of propanal. Major formed unsaturated hydrocarbons from *n*-pentane oxidation were 1-pentene, 2-pentene, and 1-butene.

The low temperature oxidation of *n*-hexane in a flow reactor was studied by Mével et al [28]. The study conditions were equivalence ratios of 0.7, 1 and 1.5 for mixtures diluted at 90% with nitrogen, pressure at 1 bar, and over the temperature range 450 – 1000 K. The main production of alkenes was observed at intermediate temperature (< 1000 K) and for the studied rich condition of φ= 1.5. Zhang et al. [29] measured the concentration of intermediate species during the oxidation process of *n*-hexane in a JSR over a wide temperature range of 530–1160 K, at pressure 10 atm, and for equivalence ratios of ϕ=0.5, 1.0 and 2.0. At the lean condition of ϕ=0.5, the formation of oxygenated hydrocarbons has taken place generally at low to intermediate temperature of 600-900 K, and the C_2-C_5 *n*-alkenes have been maximally formed at intermediate temperature around 800-900 K. The stoichiometric oxidation of the isomers of hexane was studied using a JSR at a constant pressure of 1.06 bar and temperatures ranging from 550 to 1000 K by Wang et al. [30]. At low temperature (< 800 K), *n*-hexane was the most reactive isomer. Its oxidation products of alkanes (methane, ethane and propane) and acetylene were detected around 900 K. The intermediate temperature of 800 K has favorited the production of alkenes. At low temperature of 650 K, formaldehyde, acetaldehyde, propanal, methanol, acetic acid, and acetone were mainly formed.

The stoichiometric oxidation of *n*-heptane was investigated under the JSR combustion conditions of temperature range 500–1100 K and at a pressure of 800 Torr (1.06 bar) by Herbinet et al. [21]. The formation of methane, ethane and C_2-C_6 alkenes and acetylene was observed around the intermediate temperature of 850 K. But the maximum production of ethene, propene, formaldehyde, methanol, acetaldehyde, propanal, acetone, acetic acid, 1-butene, 1-pentene, 1-hexene, heptenes isomers, 2-ethyl-5-methyl-tetrahydrofuran, 2,4-dimethyloxetane and diones, was detected at low temperature 600-650 K. Herbinet et al. [31] presented a simulated time evolution of the mole fractions of the fuel (75% *n*-heptane/25% *iso*-octane mixture in air at ϕ= 0.3) and of five membered ring cyclic ethers in an HCCI engine. The main

cyclic ethers were formed during the low temperature reaction before ignition. These organic compounds were completely consumed during auto-ignition. A zero-dimensional numerical study of the chemical reaction kinetics of *n*-heptane in an HCCI engine was effectuated by Zheng et al. [32] using a detailed chemistry. It concluded that formaldehyde and hydrogen peroxide were important products at low temperature chemistry. The converting of formaldehyde to carbon monoxide took place at high temperature which was controlled by hydrogen peroxide decomposition. The stoichiometric low temperature combustion of *n*-heptane in a high-pressure JSR was investigated experimentally by Dagaut et al. [33] in a wide range of conditions, temperature 550 - 1150 K, and pressure 10 - 40 atm. It has been concluded that raising the pressure boosted the decomposition of hydrogen peroxide, which is pressure dependent, and then the influence of OH reactions at lower temperature becomes more significate. Hence, shifting the high-temperature oxidation towards lower temperatures at high pressure could produce a reduction of the negative temperature coefficient (NTC) region. Therefore, the formation of low-temperature products at high pressure did not moderate, as temperature rises, fast as observed at low pressure [33]. This observation could be generally interesting for our study of *n*-alkanes converting under pressure raising conditions of HCCI combustion process.

It could be concluded from the literature study that LIT chemistry region consists of the more favourite conditions to produce our target species (oxygenated hydrocarbons, hydrogen peroxide, formaldehyde, and alkenes) from C_4-C_7 *n*-alkanes oxidation. Alkenes could be even produced at more high temperature. The RG and EGR can be sources of cycle-to-cycle variability in HCCI engines but also can be used to improve engine performance and operating conditions. Therefore, this modeling work investigates the use of an HCCI combustion process as a reactor to generate reactive or intermediate useful species from *n*-alkanes LIT reaction. The study carries out a number of sweeps of engine operating conditions in order to assess trade-offs between work, reaction time and oxidizer availability, and target species formation. The study also touches on the cyclic variability of sequential combusting cycles and the feedback between previous-cycle residual gasses and the auto-ignition behaviour of the following cycle.

Chapter 2 presents the modelling tools and conditions with describing the methodology of this exploring study. In order to classify and highlight some important results of this work, chapter 3 of results and discussion is subdivided into three chapters of *n*-butane conversion, C_5-C_7 *n*-alkanes conversion and the general one of low-intermediate temperature products of *n*-alkanes. Finally, a conclusion is presented in chapter 4.

MODELLING AND METHODOLOGY

A numerical simulation of an HCCI engine was performed using a homogeneous single-zone reactor with detailed elementary reaction mechanisms and heat transfer to the cylinder walls. It's completely true that in real combustion systems, temperature stratification exists, leading to significantly more drawn-out heat release events than are observed in single-zone model, which makes the predicting of ignition and emissions formation using single-zone model non accurate especially for high temperature conditions [8, 34]. As the interest of this paper is on the formation of such reactive species of oxygenated hydrocarbons, hydrogen peroxide, formaldehyde and alkenes which occurs mainly at LIT chemistry conditions where no ignition takes place, consequently the use of single-zone model was considered quiet useful as a first-order approximation for the prediction of the more favourite operating conditions to produce the target species.

The software package CANTERA [35] was used with Aramco's detailed reaction mechanisms for the oxidation of C_1 – C_4 alkanes of Li et al. [36], pentane isomers of Bugler et a. [26], *n*-hexane of Zhang et al. [29] and *n*-heptane of Zhang et al. [37]. These mechanisms have been selected for their wide range of validation covering generally high pressures (operation of an HCCI engine), low (domain of this work interest) to high temperatures, and lean to rich conditions for equivalence ratios. As in reality, there are no total predictive kinetic mechanisms, the experimental validation of any modeling study still an obligation. Table 1 presents the basic parameters of the engine simulation, which is available at the Institute for Combustion and Gas Dynamics of Duisburg-Essen university for perspective experimental validation of this work results.

The model uses the CANTERA reactor library of a single cylinder of a four-stroke engine. It simulates the closed-valve

Table 1: Engine properties and operating parameters. The crank angle convention is that gas-exchange TDC is 0° crank angle (CA).

Displacement	332 cm^3
Bore / stroke	65 / 100 mm
Con. rod length	200 mm
Comp. ratio (*Cr*)	3 – 15
Engine speed (*Es*)	100 – 2000 rpm
Intake temperature	350 – 450 K
Intake open/close	18 / 198°CA
Exhaust open/close	522 / 18°CA

portion of the cycle (essentially compression and expansion), discretizes the piston motion into small increments, and consists of the following steps: At exhaust valve closing, the mass, temperature, and composition of the RG from the previous cycle is registered. At intake valve closing, the cylinder volume is filled with that product gas, plus fresh charge at intake conditions. The valves objects of Cantera assumed that RG and fresh charge are mix instantaneously. In the first cycle, only fresh charge is filled in (No RG). Heat transfer to the walls was estimated by Newton's law of cooling and Woschni's correlation presented in CHEMKIN Theory Manual [38] and thus this model default parameters are adopted in CANTERA. The used heat transfer model and parameters were validated in our work [15].

To explore a wide range of main operating conditions that influence the sensitive and decisive LIT thermochemistry of lean *n*-alkanes/air mixtures in combustion, it has been varied compression ratio from 3 to 19, engine speed from 100 to 2000 rpm and equivalence ratio from 0.05 to 1 at fixed intake temperature and pressure of 400 K and 1 bar. This exploration study of favourite operating conditions of compression ratio (*Cr)*, engine speed (*Es),* and equivalence ratio (φ) to produce oxygenated hydrocarbons, hydrogen peroxide, acetaldehyde and/or alkenes has followed the strategy of the three following steps proposed by Saylam et al. [15] to identify the near optimal operating conditions of maximum target species production:

1. Estimating the optimal *Cr*, by varying it from 3 to 19 and choosing that of maximum yields production, needed to suitably increase the reactivity of fuel-air-mixtures at otherwise fixed conditions, here *Es* = 600 rpm, φ = 0.25, T_{in} = 400 K, and p_{in} = 1 bar.
2. At this near optimal *Cr*, *Es* is now varied from 100 to 2000 rpm in order to find the close reaction time appropriated to generate the highest yields of the target species.
3. At now fixed *Cr* and *Es,* φ is then varied in the range of 0.05 - 1 to get the near optimal φ.

In principle, this sequence would be very helpful to find even the optimal conditions using an optimization algorithm, but instead we will be satisfying to find the more favourite/near optimal conditions to produce the target species.

RESULTS AND DISCUSSION

Conversion of *n*-butane

For *n*-butane as the fuel and two different compression ratios (*Cr)*, 5 and 10, twenty successive cycles were generally simulated. Figure 2 shows the yield (the product species mass, Y_p, divided by the initial mass of fuel, Y_0, in percentage, expressed in the following equation) of key reactive species and the temperature at the end of each of the 20 simulated cycles.

$$Yield = 100\frac{Y_p}{Y_0}$$

Also the maximum temperature in each cycle is included. The intake temperature and pressure (T_{in}, p_{in}) were 400 K and 1 bar respectively, the engine speed (*Es)* was 600 rpm, and the equivalence ratios (ϕ) was 0.25. At low compression ratio of 5, Figure 2a, the system gradually approached steady state, but large cycle-to-cycle variations were found for the high compression ratio of 10, Figure 2b. For such cases, the concentration of hydrogen peroxide, formaldehyde, methanol, and ethene increases for a certain number of cycles before a cycle with ignition and complete consumption of these intermediate species occurs. The RG

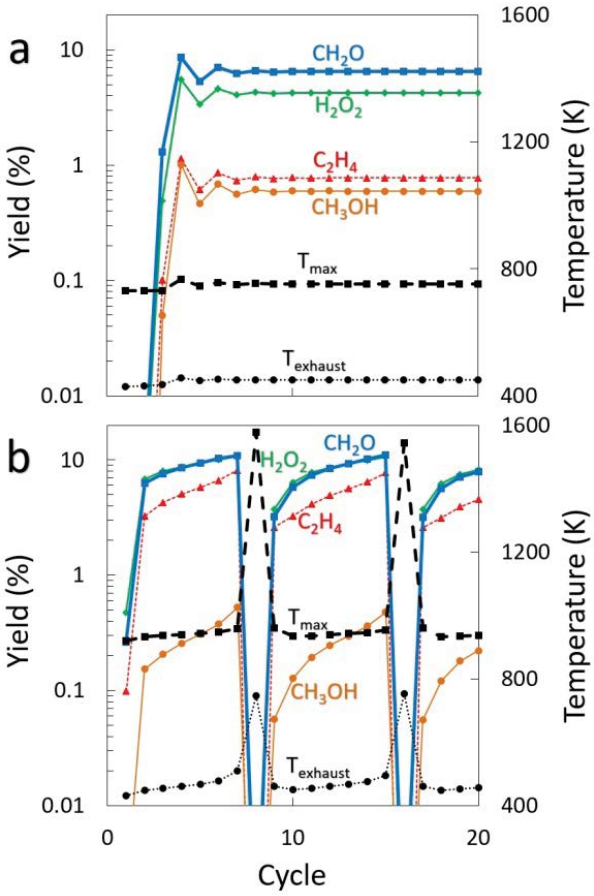

Figure 2: Cycle-to-cycle variations of exhaust composition and temperature and the maximum temperature. *N*-butane oxidation at (a) *Cr* = 5, and (b) *Cr* = 10. T_{in} = 400 K, p_{in} = 1 bar, *Es* = 600 rpm, and φ =0.25.

from the previous cycle influences the starting temperature and composition in a given cycle, which affects the mixture reactivity and then the cycle-to-cycle variability.

The degree of chemical conversion depends on the balance between mixture reactivity and available time. For the case *Cr*= 5, the low compression of fuel-air mixture produced reactive species but was not able to generate enough heat release for cycle-to-cycle variations. Figure 3a and b show that these reactive species, in particular hydrogen peroxide and 1-butene for these conditions, were formed principally at mass fractions of several percent at low to intermediate temperatures during the maximum mixture reactivity attended near to TDC and survive the cycle when auto-ignition is avoided. In the following, we aimed to find conditions with minor cycle-to-cycle variations, but relatively high yields of chemicals/synthetic fuels like oxygenated hydrocarbons, hydrogen peroxide, formaldehyde or alkenes. For further analysis, we averaged the exhaust composition, peak temperatures and the indicated mean effective pressure (IMEP) over the last 10 of the 20 simulated cycles, these cycles representing steady-state operation, and calculated the standard deviation as a measure of remaining cycle-to-cycle variability.

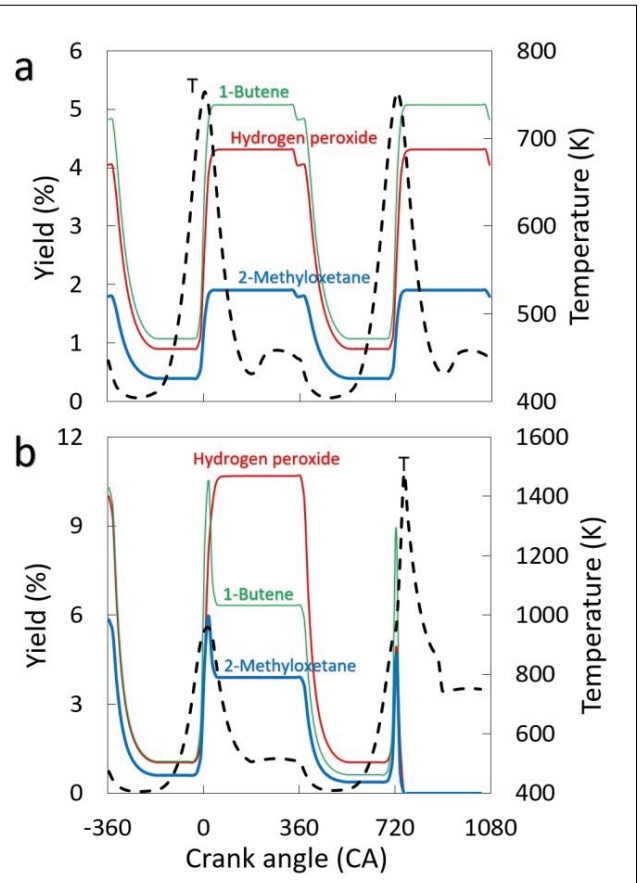

Figure 3: Influence of cycle-to-cycle variations on exhaust composition and mixture temperature. Conditions are the same as in Figure 2.

Figures 4 shows the results for *n*-butane when varying *Cr* from 3 to 19, *Es* from 100 to 2000 rpm, and φ from 0.05

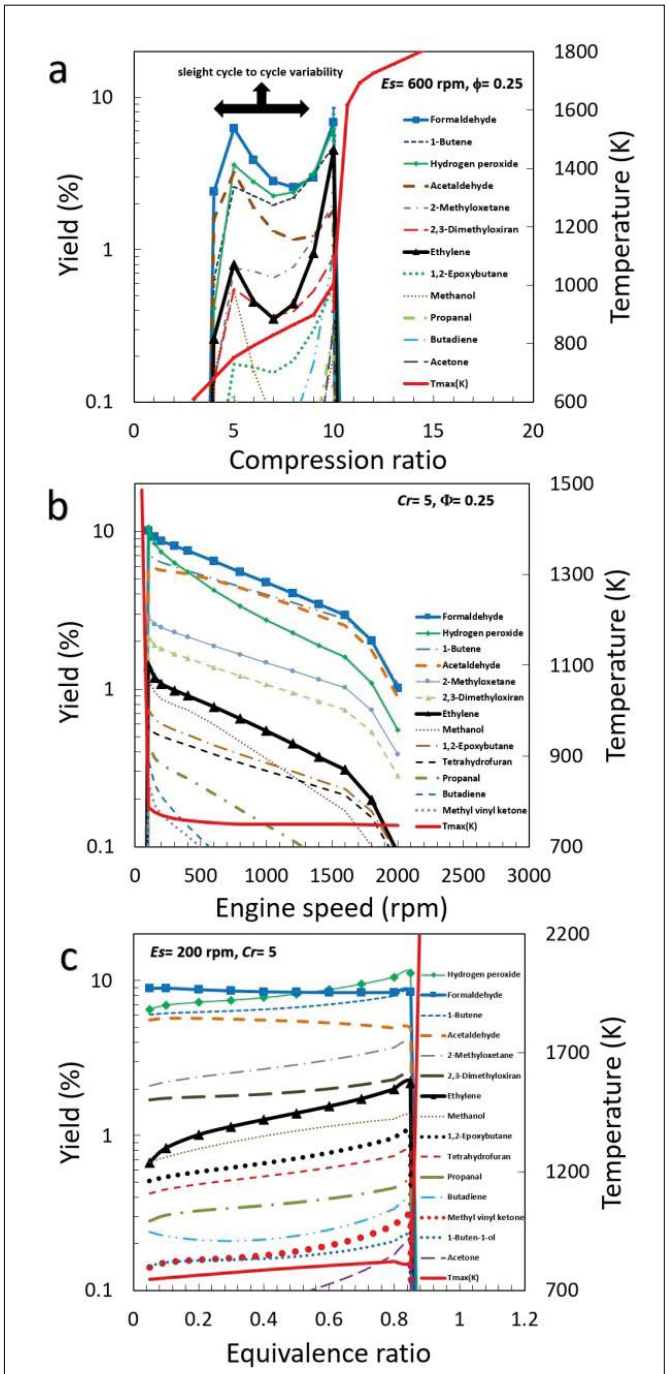

Figure 4: *N*-butane oxidation exhaust products and cycle-maximum temperature as a function of (*a*) compression ratio *Cr* at *Es*= 600 rpm and φ =0.25, (*b*) engine speed *Es* at *Cr=5* and φ =0.25, and (*c*) equivalence ratio φ at *Es*= 200 rpm and *Cr=5*. T_{in} = 400 K, p_{in} = 1 bar.

to 1, while the intake temperature and pressure were kept constant at 400 K and 1 bar, respectively. The plotted values are averages over the last 10 of the simulated 20 cycles, the 'error' bars indicating the standard deviation (SD) when significant cyclic variability was present, here SD≅ 1 - 3 for target species and 190 for cycle-maximum temperature at only *Cr*= 10. Figure 4a shows that for our initial guess of *Es* = 600 rpm and φ = 0.25, important formaldehyde, 1-butene, acetaldehyde, hydrogen peroxide and C_2-C_3 cyclic ethers formation was observed for the range of compression ratios 4 – 10, which corresponds to the range of cycle-maximum temperature from around 680 K to near 1000 K. All other target species were produced in even lower concentrations. At lower *Cr*, the reactivity of *n*-butane-air mixture is not enough to produce significant yields of target species, and even at higher *Cr*, this production is poor because of the enhanced auto-ignition of mixture in combustion that consumes the most of these reactive species. The influence of the region of negative temperature coefficient (NTC) on the production of target species manifested clearly in the range of compression ratio of 5 to 10, which consistent to the range of cycle-maximum temperature of near 750 to around 1000 K. The overall reaction rate decreased passing from cycle-maximum temperature of near 750 K to around 830 K. It corresponds to a transition in the oxidation chemistry from the low temperature to intermediate temperature reaction regime [39].

In spite of the higher productivity of target species at *Cr* = 10, it has been chosen the *Cr* = 5 that yielded slightly less of products but with relatively very low cycle to cycle variability, SD≅ $5e^{-3}$ for target species and $3e^{-2}$ for cycle-maximum temperature, important for a stable production. An interesting observation: when choosing a low cycle-to-cycle variability condition, here *Cr* = 5, for a following study such varying the equivalence ratio at the fixed *Es* and *Cr*, generally, low cycle-to-cycle variability was obtained regarding that of using a high cycle-to-cycle variability condition, here *Cr* = 10. At this chosen *Cr* = 5, the fuel was converted to mass yield about 6.5% of formaldehyde, 5% to acetaldehyde and the same to 1-butene, and 4% to hydrogen peroxide. Ethene and C_2-C_3 cyclic ethers were formed with yields about 1% each. Now at this optimal, *Cr* = 5, the engine speed has been varied. The results in Figure 4b were consistent with those for varying *Cr*. As speed was increased from 100 to 2000, the maximum temperature was reduced from near 790 K to around 750 K and thus escorted with modest dropping in production yields, the latter corresponding to low-reactive compression, because the reaction time for high engine speed is not long enough to produce significant concentrations of target species. Generally, the output of intermediate species in the exhaust dropped towards lower speed, here (< 100 rpm), because there was enough time for hot ignition which should be avoided, cycle-maximum temperature (>1500 K). The highest values of formaldehyde, hydrogen peroxide, 1-butene and acetaldehyde mass yield now were 10%, 10%, 7% and 6% respectively, at an engine speed of 100 rpm, with the advantage that the cyclic variability was very low, SD≅ $1e^{-5}$. It has chosen the near value of 200 rpm for the farther study of equivalence ratio varying to avoid the use of the critical engine speed of 100 rpm. Now equivalence ratio was varied at *Es* = 200 rpm and *Cr* = 5. The results in Figure 4c show that now the hydrogen peroxide, formaldehyde, 1-butene, acetaldehyde, ethene, C_2 cyclic ethers (oxiranes), C_3 cyclic ethers (oxetanes), and C_4 cyclic ethers (furans) yields, of 11%, 8.4%, 8%, 5%, 2.2%, 2.4%, 3.9, and 0.8 respectively, increased up to the richest investigated conditions of φ = 0.85, where the temperature increased but remain relatively low, around 825 K. No significate yield, up to 0.1%, of acetic acid was predicted as it was detected by Herbinet et al. [16, 17] from the oxidation of a stoichiometric *n*-butane/oxygen/argon mixture in a JSR under quasi-atmospheric pressure. A large tray of more lean conditions from φ = 0.8 until 0.05 favorited a slight decreasing in yields of target species, accompanied with decreasing of temperature to around 750 K. Richer conditions enhanced higher reactivity of *n*-butane/air mixture leading to a point of auto-ignition regime, with maximum temperatures higher than 2200 K, and then to the quasi full consumption of the reactive target species. As Indicated Mean Effective Pressure (IMEP) represents the work delivered to the piston over the compression and expansion strokes, per cycle per unit displaced volume. The intermediate reactivity of *n*-butane/air mixture in combustion without attending the auto-ignition regime resulted negative IMEPs or very modest positive values. For the range of = 0.05 to 0.8, and at *Es* = 200 rpm and *Cr*= 5, the target products from *n*-butane combustion were formed with IMEP = -0.2 to 0.45, respectively.

Conversion of C_5 – C_7 *n*-alkanes

Figure 5 presents the most important results from the corresponding investigation with *n*-pentane (C5), *n*-hexane (C6) and *n*-heptane (C7) as the fuels. In terms of the compression ratio and engine speed, similar behaviours as for *n*-butane were observed for the three fuels. But tighter concave-down zones of NTC behaviour were observed for the productive compression ratio ranges of *n*-pentane, *n*-hexane and *n*-heptane, where *n*-butane showed a distinguished concave-up of NTC behaviour, figure 4a.

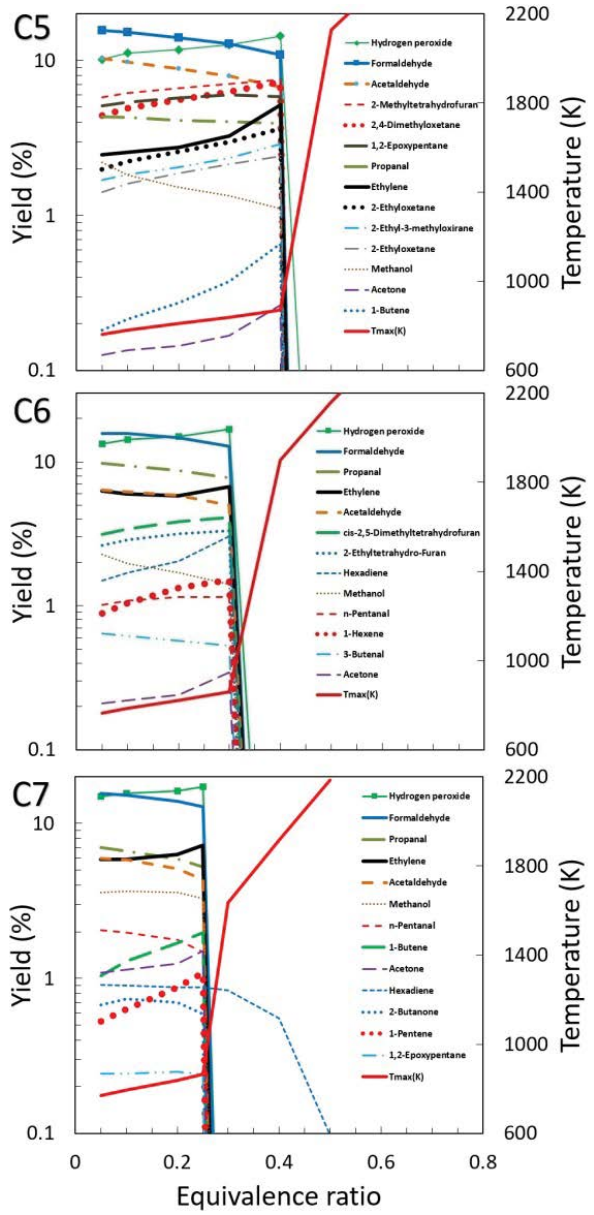

Figure 5: C_5-C_7 *n*-alkanes oxidation exhaust products and cycle-maximum temperature as a function of equivalence ratio φ. *Cr=5*, *Es*= 400 rpm, T_{in} = 400 K and p_{in} = 1 bar.

These tighter ranges of concave-down of NTC behaviour for C_5-C_7 *n*-alkanes consist to the zones of system reactivity raising in their NTC region started at cycle-maximum temperature around 815, 830 and 845 K, respectively, while the concave-up behaviour of *n*-butane started at 750 K of system reactivity reduction zone. The ranges of productive compression ratio were tighter when passing toward the long-chain, more reactive, *n*-alkanes. These limited and tight ranges in compression ratio to produce our target species from C_5–C_7 *n*-alkanes are due to the much higher reactivity of fuels but also to the formation of intermediate reactive species – hydrogen peroxide, formaldehyde, alkenes, and oxygenated hydrocarbons – which are very sensitive to the temperature and pressure history. Therefore, the accumulation of these reactive species, figure 2b, produced during the maximum mixture reactivity attended near to TDC, figure 3, in the RG over several cycles increases the reactivity of the mixtures in compression which feeds the cycle-to-cycle variability, and thus increases the heat release rate for the richer conditions, to achieve a critical point of system auto-ignition which must be avoided here. The selection of the optimal compression ratio or engine speed conditions has always followed the rule of choosing the one of maximum productivity with minimum cycle-to-cycle variability.

For *n*-pentane, an optimal compression ratio of *Cr*= 5 was required with a selected engine speed of 400 rpm near to the maximum productive but critical one of 300 rpm, as discussed for *n*-butane. The optimal productive compression ratio and engine speed for *n*-hexane and *n*-heptane were also 5 and 400 rpm, respectively, as for *n*-pentane. Therefore, it was interesting to test the dual *Cr* = 5 und *Es*= 400 rpm, not shown, for the variation of equivalence ratio concerning the *n*-butane. The obtained behaviour was generally the same with less yields of products, yields decreasing in the range of 5% – 65% depending on the specie, but through the advantage of extending the range of productive equivalence ratio to reach the stoichiometric limit of this study. As the engine speed was increased from 100 to 2000 rpm, production yields dropping was less than observed in figure 4b of *n*-butane. As the chain of *n*-alkanes, C_5-C_7 is longer, slighter influence of engine speed on production yields was detected. The higher reactivity of these *n*-alkanes compensates the reduction in reaction time necessary to produce significant concentrations of the target species.

Generally, as seen in Figure 5, the maximum yield of target species were observed at the productive ranges of equivalence ratio from the leanest studied condition of φ = 0.05 until 0.4, 0.3 and 0.2 and at *Es* = 400 rpm and *Cr* = 5 for *n*-pentane, *n*-hexane and *n*-heptane as fuels, respectively. But richer fuel-air mixtures lead to the non- favourite production condition of target species characterized by the auto-ignition of mixture in oxidation, which corresponds to a critical high reactive range of equivalence ratio for at least one of the prefixed operating conditions of *Es* = 400 rpm and *Cr* = 5. The cycle-maximum temperatures to produce maximum concentrations of target species were situated, for the C_5-C_7 *n*-alkanes as for *n*-butane, around the limit of low to intermediate temperature of 820 40 K. The production

of alkenes observed in literatures at higher temperature was also predicted here for hexadiene from *n*-heptane oxidation. Its production continued until the richest conditions of 0.5 where the cycle-maximum temperature attended near 2200 K. The IMEP values for the productive ranges of equivalence ratio of the target's species from the C_5-C_7 *n*-alkanes were situated in the range of -0.18 to 0.38 where there was no-ignition.

The oxidation of *n*-pentane produced yields at φ = 0.4 of 14.4% hydrogen peroxide, 11%formaldehyde, 6.8% acetaldehyde, 5.2% ethene, 3.5% C_2 cyclic ethers, 10.9% C_3 cyclic ethers, and 7.5% C_4 cyclic ethers. These results are generally in good agreement with the sequence of major species detected experimentally by Kang et al. [14] of *n*-pentane oxidation under motored engine conditions of T_{in}= 393 K, *Es*= 600 rpm, and ϕ= 0.25. The general sequence of major species detected by Zhang et al. [29] in a JSR for the lean condition of ϕ=0.5 and at *p*= 10 atm is also in good agreement with the predicted yields from *n*-hexane oxidation in this study, where 16.9% hydrogen peroxide, 12.8%formaldehyde, 6.7% ethene, 5% acetaldehyde, 7.7% propanal, 1.54% 1-butene, 7.5% C_4 cyclic ethers, 1.2% C_2 cyclic ethers, and 0.18% C_3 cyclic ethers were formed for φ = 0.3. At φ = 0.25, *n*-heptane oxidation produced 17.3% hydrogen peroxide (H_2O_2), 12.8%formaldehyde (CH_2O), 7.2% ethene (C_2H_4), 4.3% acetaldehyde (CH_3CHO), 5.2% propanal (C_2H_5CHO), 3.8% butanal (C_3H_7CHO), 1.5% *n*-pentanal (C_4H_9CHO), 3.3 methanol (CH_3OH), 3.5% *n*-heptene isomers (C_7H_{14}), 2% 1-butene (1-C_4H_8), 1.5% acetone (CH_3COCH_3), 0.25% 1,5-hexadiene (C_6H_{10}), 1% C_2 cyclic ethers (oxiranes), 3.7% C_3 cyclic ethers (oxetanes), and 6.6% C_4 cyclic ethers (furans) yields. The LIT chemistry of C_5-C_7 *n*-alkanes predicted low yields (< 0.1%) of aromatics (benzene, and phenol), C5 cyclic ethers (tetrahydropyran, and 2-ethyloxane), acids (acetic acid, propanoic acid, and 4-methylpentaneperoxoic acid), hydroperoxides (3-pentyl hydroperoxide , phenyl hydroperoxide, hexyl hydroperoxides, 2-hydroperoxyhexane, heptyl hydroperoxide, and 1-methylhexyl hydroperoxide) and diones (benzoquinone, heptane-2,4-dione, 3-oxoheptanal, heptane-3,5-dione, cyclohexa-3,5-diene-1,2-dione, and cyclohexa-2,5-diene-1,4-dione).

Low-intermediate temperature products of *n*-alkanes

The near optimal operating conditions and the corresponded major products, yields up to 0.1%, of LIT chemistry from C_1-C_7 *n*-alkanes fuelled an HCCI combustion process at T_{in}= 400 K and p_{in}= 1 bar are collected in table 2. The results concerning C_1-C_3 *n*-alkanes were acquired from the work of Saylam et al. [15]. The maximum production of target species from the lower reactive C_1-C_3 alkanes required relatively high compression ratios (*Cr* = 13 for methane, 11 for ethane and 9 for propane) to enhance enough fuel-air mixture reactivity with avoiding the full auto-ignition regime. A constant *Cr* = 5 was sufficient to boost the goal of balanced reactivity for the longer-chain of C_4-C_7 *n*-alkanes. The engine speed of 400 rpm was the optimum for all C_1-C_7 *n*-alkanes. The latter emphasizes again the low sensitivity of *n*-alkanes, especially the long-chain ones, to reaction time

Table 2: Near optimal productive operating conditions and yields of LIT chemistry products from C_1-C_7 *n*-alkanes fuelling an HCCI engine at T_{in}= 400 K and p_{in}= 1 bar.

Characteristics \ *n*-alkane		C_1	C_2	C_3	C_4	C_5	C_6	C_7
Near optimal productive operating conditions at T_{in} = 400 K and p_{in} = 1 bar	*Cr*	13	11	9	5			
	Es	400						
	φ	0.05	0.15	0.15	1	0.4	0.3	0.25
	Cycle-maximum temperature (K)	1040	960	895	780	870	860	860
Yields%	Total useful converting	17.6	2.7	1.8	36	67	81	85
	H_2O_2	3.4	0.43	0.6	6.6	14.4	16.9	17.3
	CH_2O	13.3	0.23	0.6	8	11	12.8	12.8
	C_2H_4	0.34	2	0.47	1.55	5.2	6.7	7.2
	CH_3CHO	-	-	0.11	6	6.8	5	4.3
	CH_3OH	0.5	-	-	1.7	1.1	1.4	3.3
	1-C_4H_8	-	-	-	5.9	0.65	1.54	2
	C_2 cyclic ethers	-	-	-	1.66	3.5	1.2	1
	C_3 cyclic ethers	-	-	-	2.6	10.9	0.18	3.7
	C_4 cyclic ethers	-	-	-	0.55	7.5	7.5	6.6
Reference		[15]			This work			

for the production of LIT chemistry species. This matter was presented and discussed in paragraph 3.2. The *n*-butane, as an intermediate alkane between the low and high-reactivity *n*-alkanes, showed a long range of productive equivalence ratio with a maximum productivity around the studied limit of stoichiometric, paragraph 3.1. Figure 6 presents the cycle-maximum temperature history in function of compression ratio for the C_1-C_7 *n*-alkanes at *Es*= 600 rpm, ϕ=0.25, T_{in}= 400 K, and p_{in}= 1 bar. The low temperature chemistry limit of 600 K was common at *Cr* = 3 for the C_1-C_7 *n*-alkanes, where the reactivity of studied *n*-alkanes plays very limited role, the increase in temperature is due principally to the compression of gaseous mixtures.

The optimal *Cr* = 5 for the C_4-C_7 *n*-alkanes was situated at earlier stage of the distinguished concave-up of NCT region of *n*-butane LIT chemistry production, figure 4a, and thus means the extending of favourite temperature range, from the low temperature of near 750 K at *Cr* = 5 to around 1000 K at *Cr* = 10, to produce the target species regarding that of longer-chain *n*-alkanes, which situated from the intermediate temperatures of near 815, 830, and 845 K to around 1000 K for *n*-pentane, *n*-hexane, and *n*-heptane, respectively. In consequence, the competition between the reduction of system reactivity at this earlier stage of NCT region of *n*-butane and its raising achieving richer conditions permitted the extending of the productive range of equivalence ratio of *n*-butane to include the stoichiometric. As low-reactivity the C_1-C_3 alkane has, as the optimal compression ratio becomes high and the productive ranges

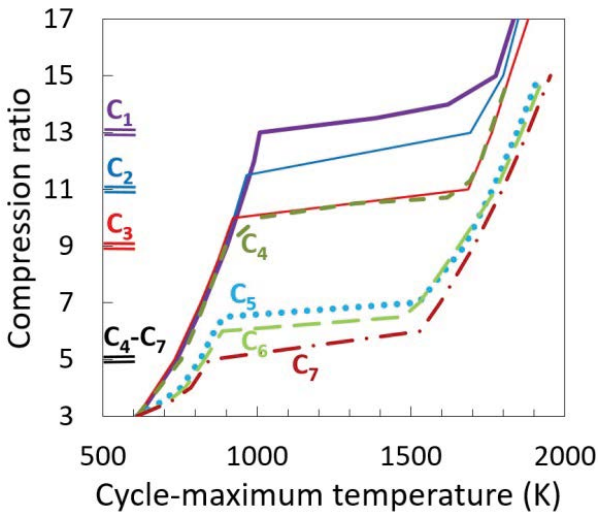

Figure 6: Cycle-maximum temperature history of C_1-C_7 *n*-alkanes oxidation in function of compression ratio *Cr*. *Es*= 600 rpm, ϕ= 0.25, T_{in} = 400 K and p_{in} = 1 bar.

of temperature convert tighter, started at near 890, 950, and 1000 K for propane, ethane, and methane, respectively. The decreasing of the optimal cycle-maximum temperatures from near 1040 to around 860 K, corresponded to optimal equivalence ratios for each *n*-alkane, in function of the long-chain of C_1-C_3 and C_5-C_7 *n*-alkanes, Table 2, is completely coherent with the requirement of intermediate balanced energy to enhance enough reactivity of fuel-air mixture without passing to auto-ignition regime. The exception of the lower value of 780 K for the maximum productivity of the stoichiometric *n*-butane/air mixture, 830 K for *Es*= 200 rpm and φ = 0.85, improves the presented argument of the competition between raising the system reactivity for richer condition and its reduction in the NCT region of *n*-butane. Considering the leanest optimal conditions of φ = 0.05 and 0.15, and the very tight compression ratio conditions to produce the target species from C_1-C_3 alkanes, the practical exploitation of such production isn't beneficial. An advantageous application could be the operating of an in-situ production unit of an HCCI cylinder to produce such high reactive species, hydrogen peroxide, formaldehyde and ethene from methane/natural gas oxidation at *Es* = 400 rpm, *Cr* = 13, T_{in} = 400 K, p_{in} = 1 bar and φ= 0.2 [15]. The exhaust of this unit could be mixed with fresh fuel to stabilize a power-producing HCCI or SI engine operation [15]. Generally, C_4-C_7 *n*-alkanes yielded important quantities, 4 - 17%, of hydrogen peroxide, formaldehyde, ethene, and acetaldehyde, but also good production, 1 – 3 % of methanol, and C_2 cyclic ethers. 1-butene was good produced, 1.54%, 2%, and 5.9%, from C_6, C_7 and C_4 *n*-alkanes, respectively. C_3 cyclic ethers were formed well, 2.6%, 3.7%, and 10.9%, from C_4, C_7 and C_5 *n*-alkanes, respectively. The C_5-C_7 *n*-alkanes yielded interesting percentage, around 7, of C_4 cyclic ethers. The production of these LIT chemistry species as chemicals or pool of reactive fuels/air mixture from C_1-C_7 *n*-alkanes, especially from long-chain *n*-alkanes, seems to be very beneficial, total yields percentages of target species are 17.6, 2.7, 1.8, 36, 67, 81, and 85 from C_1-C_7 *n*-alkanes, respectively. The concept of polygeneration is not applied here while the production of target species occurred at LITs and consequently the IMEP was generally negative or had very modest positive values, less than 1 bar.

CONCLUSIONS

The favourite operating conditions to produce LIT chemistry products (oxygenated hydrocarbons, hydrogen peroxide, formaldehyde, and/or alkenes) from *n*-alkanes fuelled an HCCI engine have been explored using zero-dimensional modeling. Important production of these compounds, as useful chemicals or synthetic fuels, is principally generated

from the early stages of the LIT chemistry of *n*-alkanes lean-combustion process. The total converting yields to produce the target species are in the range of around 2 to 85% depending of the *n*-alkane. These products are formed mainly during the maximum reactivity of fuel-air mixture attended near to TDC and survive the cycle when auto-ignition is avoided.

Even at LITs combustion conditions, the intermediate reactive species as hydrogen peroxide, formaldehyde, alkenes, and oxygenated hydrocarbons, which are very sensitive to the temperature and pressure history, could be accumulated in the RG over several cycles. This leads to increase the mixture reactivity in compression and thus to feed the cycle to cycle variability until achieving a critical point of system auto-ignition. The favourite conditions to attend such transition are low speed engine, high compression ratio and the richer conditions, which we must avoid to guarantee the production of these species mixture.

The long-chain *n*-alkanes of C_4-C_7 require a fixed low Cr = 5 to produce high concentrations of target species. Boosting the goal of enhancing enough fuel-air mixture reactivity with avoiding the full auto-ignition regime is attended for the lower reactive C_1-C_3 alkanes at relatively high compression ratios of Cr = 13 for methane, 11 for ethane, and 9 for propane [15]. As the chain of *n*-alkanes is longer, the engine speed has slighter influence on the production yields of LIT chemistry species. The optimal engine speed of 400 rpm is acquired for all C_1-C_7 *n*-alkanes. The intermediate reactivity of *n*-butane between the studied C_1-C_7 *n*-alkanes fulfils its maximum productivity of target species to be attended even around the stoichiometric. The lower and higher-reactivity of other *n*-alkanes require leaner conditions for such maximum production. This matter refers to the availability of earlier extended CNT conditions for *n*-butane production of target species. Delayed and relatively tight zones of these CNT conditions are only available for the other studied *n*-alkanes.

Avoiding the auto-ignition of high temperature chemistry in an HCCI engine gives rise to low or even to negative power "generated" from the engine, shown in this work. Consequently, the polygeneration concept for *n*-alkanes LIT chemistry production of species is not relevant here.

This modeling study focused on the identification of promising conditions to produce significant concentrations of LIT chemistry species from *n*-alkanes that need certainly to be validated experimentally, and to be exploited in the future for chemicals/synthetic fuels production and HCCI engine improvement studies. Perspective multi-zone model study, coupled with CFD simulation and/or experimental evaluation of temperature distribution inside the engine cylinder, are desired to get more accreted results considering the effect of temperature stratification in engine cylinder on chemical conversion and mixture ignition.

ACKNOWLEDGEMENTS

A. Saylam is supported by a mutual fellowship from Philipp Schwartz Initiative of the Alexander von Humboldt Foundation and Duisburg-Essen university (Germany).

REFERENCES

1. Maurya RK, Saxena MR, Yadav R, Rathore A, (2018) Numerical Investigation of Syngas Fueled HCCI Engine Using Stochastic Reactor Model with Detailed Kinetic Mechanism, in. (SAE Int. J. Engines).
2. Yao MF, Zheng ZL, Liu HF (2009) Progress and recent trends in homogeneous charge compression ignition (HCCI) engines, Prog. Energy Combust. Sci., 35 398-437.
3. Chen R, Milovanovic N (2002) A computational study into the effect of exhaust gas recycling on homogeneous charge compression ignition combustion in internal combustion engines fuelled with methane, Int. J. Therm. SCI., 41 805-813.
4. Agarwal AK, Singh AP, Lukose J, Gupta T (2013) Characterization of exhaust particulates from diesel fueled homogenous charge compression ignition combustion engine, J. Aerosol Sci., 58 71-85.
5. Alger T, Mangold B, (2009) Dedicated EGR: A New Concept in High Efficiency Engines, SAE Int. J. Engines, 2 620-631.
6. Chadwell C, Alger T, Zuehl J, Gukelberger R (2014) A Demonstration of Dedicated EGR on a 2.0 L GDI Engine, SAE International Journal of Engines, 7 434-447.
7. Tartakovsky L, Sheintuch M (2018) Fuel reforming in internal combustion engines, Prog. Energy Combust. Sci., 67 88-114.
8. Aceves SM, Flowers DL, Westbrook CK, Smith JR, Pitz W, Dibble R, Christensen M, Johansson B (2000) A Multi-Zone Model for Prediction of HCCI Combustion and Emissions, in. (SAE Int. J. Engines.
9. Hegner R, Werler M, Schie R, Maas U, Atakan B (2017) Fuel-Rich HCCI Engines as Chemical Reactors for Polygeneration: A Modeling and Experimental Study on Product Species and Thermodynamics, Energy Fuels, 31 14079-14088.
10. Hegner R, Atakan B (2017) A polygeneration process concept for HCCI-engines – Modeling product gas purification and exergy losses, Int. J. Hydrog. Energy, 42 1287-1297.
11. Wiemann S, Hegner R, Atakan B, Schulz C, Kaiser SA (2018) Combined production of power and syngas in an internal combustion engine – Experiments and simulations in SI and HCCI mode, Fuel, 215 40-45.

12. Banke K, Hegner R, Schröder D, Schulz C, Atakan B, Kaiser SA (2019) Power and syngas production from partial oxidation of fuel-rich methane/DME mixtures in an HCCI engine, Fuel, 243 97-103.

13. Lim EG, Dames EE, Cedrone KD, Acocella AJ, Needham TR, Arce A, Cohn DR, Bromberg L, Cheng WK, Green WH (2016) The engine reformer: Syngas production in an engine for compact gas-to-liquids synthesis, The Canadian Journal of Chemical Engineering, 94 623-635.

14. Kang D, Bohac SV, Boehman AL, Cheng S, Yang Y, Brear MJ (2017) Autoignition studies of C5 isomers in a motored engine, Proc. Combust. Inst., 36 3597-3604.

15. Saylam A, Atakan B, Kaiser S (2019) Modeling study of reactive species formation from C1–C3 alkanes in an HCCI engine, Combust. Theor. Model., 1-15.

16. Yamada H, Suzaki K, Tezaki A, Goto Y (2008) Transition from cool flame to thermal flame in compression ignition process, Combust. Flame, 154 248-258.

17. Bhasin MM, Slocum DW (1995) Methane and Alkane Conversion Chemistry, Springer US.

18. Lee JS, Oyama ST (1988) Oxidative Coupling of Methane to Higher Hydrocarbons, Catal. Rev., 30 249-280.

19. Gaffuri P, Faravelli T, Ranzi E, Cernansky NP, Miller D, d'Anna A, Ciajolo A (1997) Comprehensive kinetic model for the low temperature oxidation of hydrocarbons, AIChE J., 43 1278-1286.

20. Wang Z, Herbinet O, Hansen N, Battin-Leclerc F (2019) Exploring hydroperoxides in combustion: History, recent advances and perspectives, Prog. Energy Combust. Sci., 73 132-181.

21. Herbinet O, Husson B, Serinyel Z, Cord M, Warth V, Fournet R, Glaude PA, Sirjean B, Battin-Leclerc F, Wang Z, Xie M, Cheng Z, Qi F (2012) Experimental and modeling investigation of the low-temperature oxidation of n-heptane, Combust. Flame, 159 3455-3471.

22. Herbinet O, Battin-Leclerc F (2014) Progress in Understanding Low-Temperature Organic Compound Oxidation Using a Jet-Stirred Reactor, INT J CHEM KINET, 46 619-639.

23. Bahrini C, Herbinet O, Glaude PA, Schoemaecker C, Fittschen C, Battin-Leclerc F (2012) Quantification of Hydrogen Peroxide during the Low-Temperature Oxidation of Alkanes, J. Am. Chem. Soc., 134 11944-11947.

24. Herbinet O, Battin-Leclerc F, Bax S, Gall HL, Glaude PA, Fournet R, Zhou Z, Deng L, Guo H, Xie M, Qi F, (2011) Detailed product analysis during the low temperature oxidation of n-butane, Phys. Chem. Chem. Phys., 13 296-308.

25. Ranzi E, Cavallotti C, Cuoci A, Frassoldati A, Pelucchi M, Faravelli T (2015) New reaction classes in the kinetic modeling of low temperature oxidation of n-alkanes, Combust. Flame, 162 1679-1691.

26. Bugler J, Rodriguez A, Herbinet O, Battin-Leclerc F, Togbé C, Dayma G, Dagaut P, Curran HJ (2017) An experimental and modelling study of n-pentane oxidation in two jet-stirred reactors: The importance of pressure-dependent kinetics and new reaction pathways, Proc. Combust. Inst., 36 441-448.

27. Minetti R, Roubaud A, Therssen E, Ribaucour M, Sochet LR (1999) The chemistry of pre-ignition of n-pentane and 1-pentene, Combust. Flame, 118 213-220.

28. Mével R, Chatelain K, Boettcher PA, Dayma G, Shepherd JE (2014) Low temperature oxidation of n-hexane in a flow reactor, Fuel, 126 282-293.

29. Zhang K, Banyon C, Togbé C, Dagaut P, Bugler J, Curran HJ (2015) An experimental and kinetic modeling study of n-hexane oxidation, Combust. Flame, 162 4194-4207.

30. Wang Z, Herbinet O, Cheng Z, Husson B, Fournet R, Qi F, Battin-Leclerc F (2014) Experimental Investigation of the Low Temperature Oxidation of the Five Isomers of Hexane, J. Phys. Chem. A, 118 5573-5594.

31. Herbinet O, Bax S, Glaude PA, Carré V, Battin-Leclerc F (2011) Mass spectra of cyclic ethers formed in the low-temperature oxidation of a series of n-alkanes, Fuel, 90 528-535.

32. Zheng Z, Yao M (2006) Numerical study on the chemical reaction kinetics of n-heptane for HCCI combustion process, Fuel, 85 2605-2615.

33. Dagaut P, Reuillon M, Cathonnet M (1995) Experimental study of the oxidation of n-heptane in a jet stirred reactor from low to high temperature and pressures up to 40 atm, Combust. Flame, 101 132-140.

34. Aceves SM, Flowers DL, Martinez-Frias J, Smith JR, Dibble R, Au M, Girard J (2001) HCCI Combustion: Analysis and Experiments, (SAE International, Warrendale, PA (US); Lawrence Berkeley National Lab., CA (US).

35. David RLS, Goodwin G, Moffat HK, Weber BW (2018) Cantera: An object-oriented software toolkit for chemical kinetics, thermodynamics, and transport processes, https://www.cantera.org.

36. Li Y C.-W. Zhou, K.P. Somers, K. Zhang, H.J. Curran, The oxidation of 2-butene: A high pressure ignition delay, kinetic modeling study and reactivity comparison with isobutene and 1-butene, Proc. Combust. Inst., 36 (2017) 403-411.

37. K. Zhang, Banyon C, Bugler J, Curran HJ, Rodriguez A, Herbinet O, Battin-Leclerc F, B'Chir C, Heufer KA (2016) An updated experimental and kinetic modeling study of n-heptane oxidation, Combust. Flame, 172 116-135.

38. R. Design, CHEMKIN 10131: CHEMKIN Theory Manual, Reaction Design, (2013).

39. Wilk RD, Cohen RS, Cernansky NP (1995) Oxidation of n-Butane: Transition in the Mechanism across the Region of Negative Temperature Coefficient, Industrial & Engineering Chemistry Research, 34 2285-2297.